Draft version November 13, 2012
Preprint typeset using LaTeX style emulateapj v. 08/22/09

CONSTRAINING PRIMORDIAL MAGNETIC FIELDS THROUGH LARGE SCALE STRUCTURE

Tina Kahniashvili[1,2,3], Yurii Maravin[4], Aravind Natarajan[1], Nicholas Battaglia[1], and Alexander G. Tevzadze[5],

[1]McWilliams Center for Cosmology and Department of Physics, Carnegie Mellon University, 5000 Forbes Ave, Pittsburgh, PA 15213
[2]Department of Physics, Laurentian, University, Ramsey Lake Road, Sudbury, ON P3E 2C, Canada
[3]Abastumani Astrophysical Observatory, Ilia State University, 3-5 Cholokashvili Ave., Tbilisi, 0194, Georgia
[4]Department of Physics, Kansas State University, 116 Cardwell Hall, Manhattan, KS 66506
[5]Faculty of Exact and Natural Sciences, Javakhishvili Tbilisi State University, 1 Chavchavadze Ave., Tbilisi, 0128, Georgia

Draft version November 13, 2012

ABSTRACT

We study primordial magnetic field effects on the matter perturbations in the Universe. We do not limit analysis by considering a particular magnetogenesis scenario that assumes magnetic field generation prior to recombination. Contrary to previous studies, we limit the total magnetic field energy density and not the smoothed amplitude of the magnetic field at large (order of 1 Mpc) scales. We review several cosmological signatures, such as halos abundance, thermal Sunyaev Zel'dovich (tSZ) effect, and Lyman-α data. For a cross check we compare our limits with that obtained through the CMB faraday rotation effect and nucleosynthesis bound. The limits are ranging between 1.5 nG and 4.5 nG for $n_B \in (-3; -1.5)$.

Subject headings: primordial magnetic fields; early universe; large scale structure

1. INTRODUCTION

Observations show that galaxies have magnetic fields with a component that is coherent over a large fraction of the galaxy with field strength of order 10^{-6} Gauss (G) (Beck et al. 1996; Widrow 2002; Vallee 2004). These fields are supposed to be the result of amplification of initial weak seed fields of unknown nature. A recent study, based on the correlation of Faraday rotation measures and MgII absorption lines (which trace halos of galaxies), indicates that coherent μG-strength magnetic fields were already in place in normal galaxies (like the Milky Way) when the universe was less than half its present age (Kronberg et al. 2008). This places strong constraints both on the strength of the initial magnetic seed field and the time-scale required for amplification. Understanding the origin and evolution of these fields is one of the challenging questions of modern astrophysics. There are two generation scenarios under discussion currently: a bottom-up (astrophysical) one, where the needed seed field is generated on smaller scales; and, a top-down (cosmological) scenario, where the seed field is generated prior to galaxy formation in the early universe on scales that are large now. More precisely, astrophysical seed field sources include battery mechanisms, plasma processes, or simple transport of magnetic flux from compact systems (e.g. stars, AGNs), where magnetic field generation can be extremely fast because of the rapid rotation (Kulsrud & Zweibel 2008). Obviously, the correlation length of such a seed field cannot be larger than a characteristic galactic length scale, and is typically much smaller. In the cosmological seed field scenario, (Kandus et al. 2011), the seed field correlation length could be significantly larger than the current Hubble radius, if it was generated by quantum fluctuations during inflation. There are different options for seed field amplification, ranging from the MHD dynamo to the adiabatic compression of the magnetic field lines during structure formation (Beck et al. 1996). The presence of turbulence in cosmic plasma plays a crucial role in both of these processes. The MHD turbulence was investigated a long time ago when considering the processes in astrophysical plasma, while there is a lack of studies when addressing the turbulence effects in cosmological contexts (Biskamp 2003). At the late stages of the universe evolution the energy density present in the form of turbulent motions in clusters can be as large as 5-10% of the thermal energy density (Kravtsov & Borgani 2012). This can influence the physics of clusters (Subramanian et al. 2006), and/or at least should be modeled correctly when performing large scale simulations (Vazza et al. 2006; Feng et al. 2009). The proper accounting of the MHD turbulence effects is still under discussions (Springel 2010). Both astrophysical and primordial turbulence might have distinctive observational signatures. As we already noted above, the most direct signature of MHD turbulence is the observed magnetic fields in clusters and galaxies.

Galactic magnetic fields are usually measured through the induced Faraday rotation effect (see Vallee (2004)) and, as mentioned above, the coherent field magnitude is of order a few μG with a typical coherence scale of 10 kpc.[1] On larger scales there have been recent claims of an observed lower limit of order $10^{-15} - 10^{-16}$ G on the intergalactic magnetic field (Neronov & Vovk 2010; Tavecchio et al. 2010; Dolag et al. 2011), assuming a correlation length of $\lambda \geq 1$ Mpc, or possibly two orders of magnitude smaller (Dermer et al. 2011). An alternative approach to explain the blazar spectra anomalies has been discussed by Broderick et al. (2012), where two beam plasma instabilities were considered.[2] Although these instabilities are well tested through numerical ex-

[1] On the other hand, simulations starting from constant comoving magnetic fields of 10^{-11}G show clusters generating fields sufficiently large to explain Faraday rotation measurements Dolag et al. (2002); Banerjee & Jedamzik (2003).

[2] The recent study Arlen et al. (2012) claims that proper accounting for uncertainties of the source modeling leads to consis-

periments for laboratory plasma for a given set of parameters such as a temperature and energy densities of beams and background, its efficiency might be questioned for cosmological plasma because of a significantly different (several orders of magnitudes) beam, and background temperature and energy densities. Prior to these observations, the intergalactic magnetic field was limited only to be smaller than a few nG from cosmological observations, such as the limits on the cosmic microwave background (CMB) radiation polarization plane rotation (Yamazaki et al. 2010) and on the Faraday rotation of polarized emission from distant blazars and quasars (Blazi et al. 1999).

In present paper we consider the presence of the primordial magnetic field in the Universe and give a simplified description of its effect on the large scale structure formation. We focus on the linear matter power spectrum in order to show that even the total energy density presented in magnetic field (and as a consequence in magnetized turbulence) is small enough, its effects might be substantial, and the effect becomes stronger due to nonlinearity of processes under consideration.

It has become conventional to derive the cosmological effects of a seed magnetic field by using its spectral shape (parameterized by the spectral index n_B) and the smoothed value of the magnetic field (B_λ) at a given scale λ (which is usually taken to be 1 Mpc). In Kahniashvili et al. (2011) we developed a different and more adequate formalism based on the effective magnetic field value that is determined by the total energy density of the magnetic field. This formalism has been applied to describe two different effects of the primordial magnetic field; the CMB Faraday rotation effect and mass dispersion (Kahniashvili et al. 2010). As a striking consequence, we show that even an extremely small smoothed magnetic field of 10^{-29} G at 1 Mpc, with the Batchelor spectral shape ($n_B = 2$) at large scales, can leave detectable signatures in CMB or LSS statistics. In present investigation we have been focus on the thermal Sunyaev-Zel'dovich effect, the cluster number density, and Lyman-α data. These tests has been studied in Shaw & Lewis (2010), but again in the context of the smoothed magnetic field. We also do a more precise data analysis, and we focus on the inflation-generated magnetic fields.

The structure of the paper is as follows. In Sec. II we briefly review the effective magnetic field formalism and discuss the effect on the density perturbations. In Sec. III we review observational consequences and derive the limits on primordial magnetic fields. Conclusions are given in Sec. IV.

2. MODELING MAGNETIC FIELD INDUCED MATTER POWER SPECTRUM

A stochastic Gaussian magnetic field is fully described by its two-point correlation function. For simplicity, we consider the case of the non-helical magnetic field,[3] for which the two-point correlation function in wavenumber space is (Kahniashvili et al. 2010)

$$\langle B_i^\star(\mathbf{k}) B_j(\mathbf{k}')\rangle = (2\pi)^3 \delta^{(3)}(\mathbf{k}-\mathbf{k}') P_{ij}(\hat{\mathbf{k}}) P_B(k). \quad (1)$$

tence with a zero magnetic field hypothesis.

[3] We limit ourselves by considering the non-helical magnetic field because the density perturbations, and as a result the matter power spectrum, is not affected by the presence of magnetic helicity.

Here, i and j are spatial indices; $i, j \in (1, 2, 3)$, $\hat{k}_i = k_i/k$ is a unit wavevector; $P_{ij}(\hat{\mathbf{k}}) = \delta_{ij} - \hat{k}_i\hat{k}_j$ is the transverse plane projector; $\delta^{(3)}(\mathbf{k}-\mathbf{k}')$ is the Dirac delta function, and $P_B(k)$ is the power spectrum of the magnetic field.

The smoothed magnetic field B_λ through the mean-square magnetic field, ${B_\lambda}^2 = \langle \mathbf{B}(\mathbf{x})\cdot\mathbf{B}(\mathbf{x})\rangle|_\lambda$, where the smoothing is done on a comoving length λ with a Gaussian smoothing kernel function $\propto \exp[-x^2/\lambda^2]$. Corresponding to the smoothing length λ is the smoothing wavenumber $k_\lambda = 2\pi/\lambda$. The power spectrum $P_B(k)$ is assumed to depend on k as a simple power law function on large scales, $k < k_D$ (where k_D is the cutoff wavenumber),

$$P_B(k) = P_{B0} k^{n_B} = \frac{2\pi^2\lambda^3 B_\lambda^2}{\Gamma(n_B/2+3/2)}(\lambda k)^{n_B}, \quad (2)$$

and assumed to vanish on small scales where $k > k_D$.

We define the effective magnetic field $B_{\rm eff}$ through the magnetic energy density $\rho_B = B_{\rm eff}^2/(8\pi)$. In terms of the smoothed field, the magnetic energy density is given by

$$\rho_B(\eta_0) = \frac{B_\lambda^2 (k_D\lambda)^{n_B+3}}{8\pi\Gamma(n_B/2+5/2)}\ , \quad (3)$$

and thus $B_{\rm eff} = B_\lambda (k_D\lambda)^{(n_B+3)/2}/\sqrt{\Gamma(n_B/2+5/2)}$. For the scale-invariant spectrum $n_B = -3$ and $B_{\rm eff} = B_\lambda$ for all values of λ. The scale-invariant case is the only case where the values of the effective and smoothed fields coincide. For the causal magnetic fields with $n_B = 2$ the smoothed magnetic field value is extremely small for moderate value of the magnetic field.

We also need to determine the cut-off scale k_D. We assume that the cut-off scale is determined by the Alfvén wave damping scale $k_D \sim v_A L_S$, where v_A is the Alfvén velocity and L_S the Silk damping scale (Jedamzik et al. 1998; Subramanian & Barrow 1998). Such a description is more appropriate when we are dealing with a homogeneous magnetic field, and the Alfvén waves are the fluctuations $\mathbf{B}_1(\mathbf{x})$ with respect to a background homogeneous magnetic field $\mathbf{B}_0$ ($|\mathbf{B}_1| \ll |\mathbf{B_0}|$). In the case of the stochastic magnetic field we generalize the Alfvén velocity definition from Mack et al. (2002), by referring to the analogy between the effective magnetic field and the homogeneous magnetic field. Assuming that the Alfvén velocity is determined by $B_{\rm eff}$, a simple computation gives the expression of k_D in terms of $B_{\rm eff}$:

$$\frac{k_D}{1{\rm Mpc}^{-1}} = 1.4\sqrt{\frac{(2\pi)^{n_B+3}h}{\Gamma(n_B/2+5/2)}}\left(\frac{10^{-7}{\rm G}}{B_{\rm eff}}\right). \quad (4)$$

Here h is the Hubble constant in units of 100 km s^{-1} Mpc^{-1}.

Note that any primordial magnetic field should satisfy big bang nucleosynthesis (BBN) bounds, i.e., the total energy density of the magnetic field should not be greater than 10% of the radiation energy density. Assuming that the magnetic field energy density is not damped away by MHD processes, the BBN limit on the effective magnetic field strength, $B_{\rm eff} \leq 8.4\times10^{-7}$ G, while transferred in terms of B_λ the BBN bounds result in extremely small values for causal fields, see (Caprini & Durrer 2001; Kahniashvili et al. 2011).

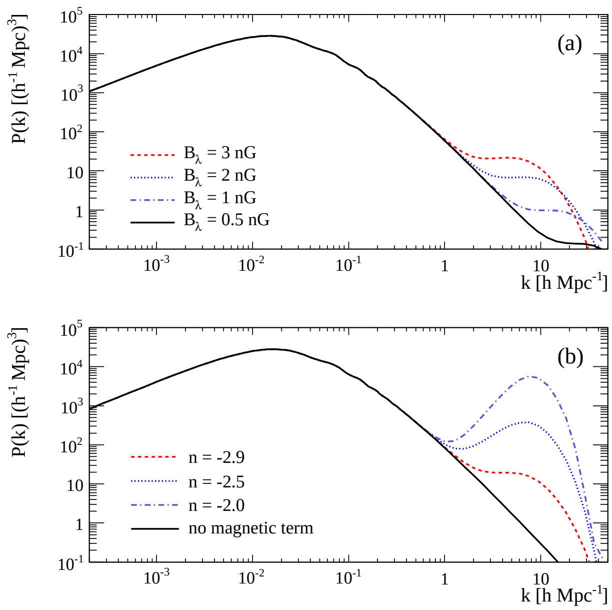

FIG. 1.— The magnetic field matter power spectra for different values of B_λ (a) and for different values of n_B (b).

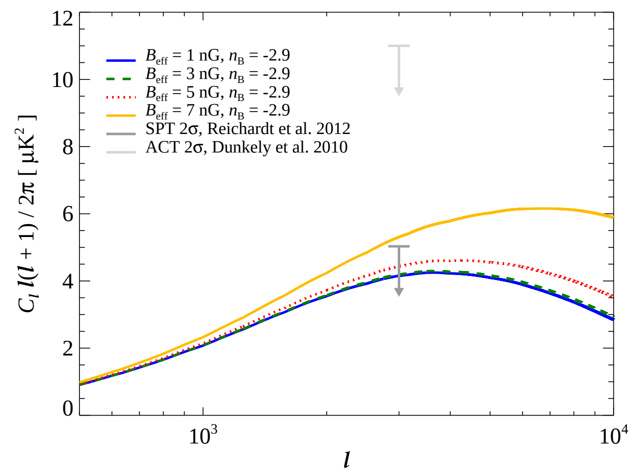

FIG. 2.— The tSZ power spectrum predictions at 150 GHz varying the primordial magnetic field model at fixed cosmological parameters, most importantly $\sigma_8 = 0.8$. These predictions are compared against the recent upper limits from ACT (Dunkley et al. 2010) and SPT (Reichardt et al. 2011) at $\ell = 3000$. The current upper limits on the tSZ amplitude at $\ell = 3000$ do not constrain the primordial magnetic field parameters $B_{\rm eff}$ and $n_{\rm B}$ as well as other observations.

The primordial magnetic field affects all three kinds of metric perturbations, scalar (density), vector (vorticity), and tensor (gravitational waves) modes through the Einstein equations. The primordial magnetic field generates a matter perturbation power spectrum with a different shape compared to the standard ΛCDM model. As we noted above in this paper we focus on the matter perturbations. As it has been shown by (Kim et al. 1996; Gopal & Sethi 2005), the magnetic-field-induced matter power spectrum $P(k)$ is $\propto k^4$ for $n_B > -1.5$ and $\propto k^{2n_B+7}$ for $n_B \leq -1.5$. This in turn affects the formation of rare objects like galaxy clusters which sample the exponential tail of the mass function. Shaw & Lewis (2010) studies in great detail the formation of the magnetic field matter power spectrum through analytical description, and provides the modified version of CAMB that includes the possibility of a non-zero magnetic field. We have used the CAMB code to determine the matter power spectra for a wide range of the magnetic field amplitudes and spectral indices. These spectra are shown in Fig. (1). It is obvious that the matter power spectrum is sensitive to the values of the cosmological parameters: the Hubble constant in the units of 100 km/sec/Mpc, h, Ω_M, and Ω_b, as well as to the density parameter of each dark matter component, i.e., $\Omega_{\rm cdm}$ and Ω_ν (here, M, b, cdm, and ν indices refer to matter, baryons, cold dark matter, and neutrinos respectively, and Ω is the density parameter. To generate the matter plot we assume the standard flat ΛCDM model with zero curvature, and we use the following cosmological parameters: $\Omega_b h^2 = 0.022$, $\Omega_C h^2 = 0.1125$, and $h = 0.71$. For simplicity, we assume massless neutrinos with three generations.[4] As we can see the increase of the smoothed field amplitude results in the additional power spectrum shift to the left, while increasing the value of n_B makes the vertical shift. As we can see the large-scale tail (small wavenumbers) of the matter power spectrum is unaffected by the presence of the magnetic field. Below we address some of effects induced by the presence of the magnetic field, especially on large scales.

[4] The standard ΛCDM model matter power spectrum $P_{\Lambda CDM}(k)$ assumes a close to scale-invariant (Harrison-Peebles-Yu-Zel'dovich) post-inflation energy density perturbation power spectrum $P_0(k) \propto k^n$, with $n \sim 1$.

3. OBSERVATIONAL SIGNATURES

Primordial magnetic fields can play a potentially important role in the formation of the first large-scale structures.

3.1. *The Thermal Sunyaev-Zel'dovich effect*

As demonstrated in Shaw & Lewis (2010) the strength of the primordial magnetic field affects the growth of structure. The power spectrum of secondary anisotropies in the CMB caused by the thermal Sunyaev-Zel'dovich effect (tSZ) is a highly sensitive probe of the growth of structure (e.g. Komatsu & Seljak 2002). The tSZ angular power spectrum probes the distribution of galaxy clusters on the sky essentially out to any redshift. At $l \simeq 3000$, half of the contribution to the SZ power spectrum comes from matter halos with masses greater than $\sim 2 \times 10^{14} M_\odot$ at redshifts less than $z \simeq 0.5$, see Battaglia et al. (2012).

All the previous work on how primordial magnetic fields affect the tSZ power spectrum used the model from Komatsu & Seljak (2002), here referred to as KS model, which has been shown to be incompatible with recent observations of clusters (Arnaud et al. 2009) and tSZ power spectrum measurements by Lueker et al. (2009). Using the KS model for primordial magnetic field studies also ignores all the recent advancements in tSZ power spectrum theory and predictions that illustrate the importance of properly modeling the detailed astrophysics of the intracluster medium (e.g. Battaglia et al. 2010, 2012; Shaw et al. 2010; Trac et al 2011). We modify

the code described in Shaw & Lewis (2010) to include these improvements by changing the pressure profile used in their model from KS to the profile given in Battaglia et al. (2010, 2012). The results from the new pressure profile are shown in Fig. (2) with the greatest difference being the amplitude of the new tSZ power spectrum is approximately two times lower than previous predictions and below the current observations constraint from ACT (Dunkley et al. 2010) and SPT (Reichardt et al. 2011) at $\ell = 3000$. Updating the theory predictions for the tSZ power significantly reduces the constraints put on primordial magnetic field parameters using these observations. In Fig. (2) we illustrate that the magnetic fields with an effective amplitude of order of 5 nG are almost excluded. Given that there is additional uncertainty in the theoretical modeling of the tSZ (e.g. Battaglia et al. 2010, 2012; Shaw et al. 2010; Trac et al 2011), combined with significant contributions from other secondary sources (Reichardt et al. 2011; Dunkley et al. 2010) around $\ell \sim 3000$, for example from dusty star forming galaxies, future tSZ power spectrum measurements are not going to be competitive in constraining primordial magnetic fields parameters.

3.2. *Halos Number Density*

The predicted halo number density $N_{\rm pred}(M > M_0, z)$ depends on the considered cosmological model. One of important characteristics of a cosmological model is the linear matter power spectrum that we reviewed in Sec. II above. Below we discuss the halo number counts dependence on the presence of the magnetic field.

The halo mass function at redshift z is $N(M > M_0, z) = \int_{M_0}^{\infty} dM\; n(M,z)$, where $n(M,z)dM$ is the comoving number density of collapsed objects with mass lying in the interval $(M, M + dM)$, and it can be expressed as

$$n(M,z) = \frac{2\rho_M}{M}\nu f(\nu)\frac{d\nu}{dM}. \qquad (5)$$

The multiplicity function $\nu f(\nu)$ is a universal function of the peak height (Press & Schechter 1974) $\nu = \delta_C/\sigma(R)$, where $\sigma(R,z)$ the r.m.s. amplitude of density fluctuations smoothed over a sphere of radius $R = (3M/4\pi\rho_M)^{1/3}$, and the critical density contrast $\delta_C \simeq 1.686$ is the density contrast for a linear overdensity able to collapse at the redshift z. Here, ρ_M is the mean matter density. For gaussian fluctuations $\nu f(\nu) \propto \exp[-\nu^2/2]$ (Press & Schechter 1974), where the normalization constant is fixed by the requirement that all of the mass lie in a given halo $\int \nu f(\nu) d\nu = 1/2$ (White 2002). The evolution of the halo mass function $n(M,z)$ is mostly determined by the z dependence of $\sigma(R,z)$.

The r.m.s amplitude of density fluctuations $\sigma^2(R,z)$ is related to the linear matter power spectrum $P(k,z)$ through (Jenkins et al. 2001)

$$\sigma^2(R,z) = \frac{D(z)^2}{2\pi^2}\int_0^{\infty} P(k,z)|W(kR)|^2 k^2 dk, \qquad (6)$$

where $D(z)$ is the growth factor of linear perturbations normalized as $D(z=0) = 1$ today, $W(kR)$ is the Fourier transform of the top-hat window function, $W(x) = 3(\sin x - x\;\cos x)/x^3$. In Fig. 3 we illustrate $\sigma(M, z = 0)$ function for the different values of the effective magnetic field, $B_{\rm eff}$, and the spectral index $n_{\rm B}$. The smaller amplitude of the magnetic field results in modifications at smaller mass scales. The $\sigma(M)$ dependence on the magnetic field characteristics is also derived in (Kahniashvili et al. 2010), but contrary to the case presented here, reflects *only* the $\sigma(M)$ induced by the pure magnetic field. In the present work we derive the effect from the magnetic field on the overall matter dispersion, including the standard density perturbations. The value of $\sigma(M)$ at $M = 2\times 10^{14} M_{\rm Sun}$ is around 0.8 that agrees well with observational data, see (Burenin & Vikhlinin 2012).

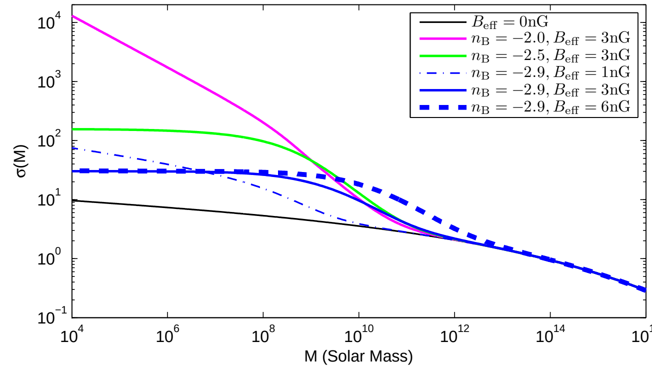

FIG. 3.— $\sigma(M, z = 0)$ for different effective magnetic field values $B_{\rm eff}$ and spectral index $n_{\rm B}$.

Numerical computation results for $n(M,z)$ are not accurately fit by the PS expression $\nu f(\nu) \propto \exp[-\nu^2/2]$, see Refs. (Sheth & Tolmen 1999; Jenkins et al. 2001; Hu & Kravtsov 2003). Several more accurate modifications of $n(M,z)$ have been proposed. Here, we use the ST modification Sheth & Tolmen (1999), as defined, (see Eq. 5 of Ref. (White 2002))

$$f(\nu) \propto [1 + (a\nu^2)^{-p}](a\nu^2)^{-1/2}\exp[-a\nu^2/2]\;, \qquad (7)$$

where the parameters $a = 0.707$, and $p = 0.303$ are fixed by fitting to the numerical results (White 2001) (for the PS case: $a = 1$ and $p = 0$) Sheth & Tolmen (1999). With this choice of parameter values the mass of collapsed objects in Eq. (7) must be defined using a fixed over-density contrast with respect to the background density ρ_M, and this requires accounting for the mass conversion between M_{180b} and M_{200c}. Such a conversion depends on cosmological parameters, see Fig. 1 of White (2001). Here, we use an analytical extrapolation of this figure to do the conversion for $\Omega_M \in (0.2, 0.35)$.

The difference induced by the magnetic field in the matter power spectrum $P(k)$ can potentially modify δ_C parameter entering in Eq. (7), that will result in different halo number counts. On the other hand, here we focus on the first order effects, so we neglect all changes induced by magnetic field in the Sheth-Tolmen model parameter fitting (see Sheth & Tolmen (1999)). We also use the halo number count function at $z = 0$ because we are focusing only on linear power spectrum, and all effects related to the magnetic field non-linear evolution (see Schleicher & Miniati (2011)) during the structure formation are neglected. We will present a more realistic scenario of the first object formation in future works.

In Fig. (4) (top panel) we illustrate the halo mass func-

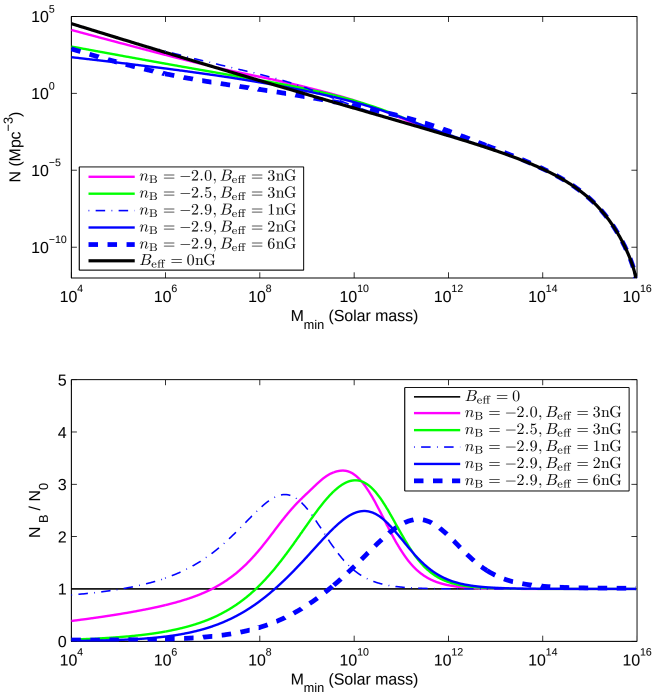

FIG. 4.— Halo number density $N(M > M_0)$ (top panel) and ratio of number density for magnetic and non-magnetic simulations $N_B)/N_0$ (bottom panel) for different effective magnetic field values B_{eff} and spectral index n_B, and $z = 0$. Number of small mass objects ($M \sim 10^4 M_\odot$) in magnetized case can be reduced down by factor of 100 compared to the non-magnetic number, object number count excess occurs for objects with mass around ($M \sim 10^{10} M_\odot$).

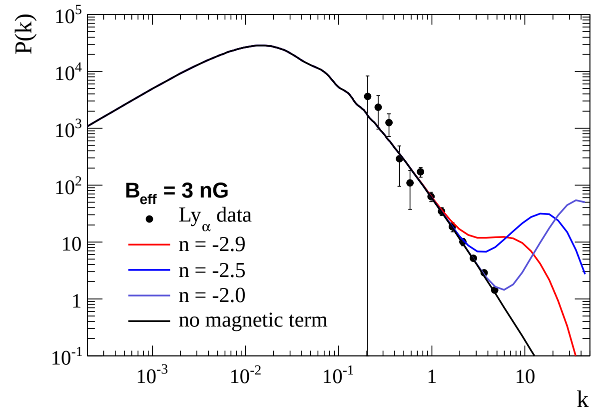

FIG. 5.— The magnetic field matter power spectra for different values of n_B and data points from Croft (2002)

tion today ($z = 0$) for different values of B_{eff} and n_B. As we can see, the magnetic field presence affects the small mass ranges, reducing the abundance of the low mass objects. We do not present here any statistics using halo data accounting for several uncertainties involving clusters physics (Battaglia et al. 2012). On the other hand, we would like to underline that the presence of high enough magnetic field might be a possible explanation of the low mass objects abundance, which is one of the unsolved puzzles in ΛCDM cosmologies.

To get a better understanding of the magnetic field influence on the halo abundance, we plot the ratio of halo number density of ΛCDM models with and without magnetic fields (see Fig. 4, bottom panel). In the high mass limit all magnetized λCDM models predict slightly (a relative difference of the order of 10^{-5}) higher halo number density. Number density excess peaks around halos with mass ($M \sim 10^{10} M_\odot$) and is strongly affected by the effective magnetic field value, as well as on the spectral shape. In contrast, at low mass limit $M < 10^7 M_\odot$, number of objects can be significantly lower as then its non-magnetic value.

3.3. *Lyman-α data*

The small scale modifications induced by the primordial magnetic field must be reflected in the first object formation in the Universe, i.e., the objects at high redshifts. The most important class of such objects are damped Lyman-α absorption systems.[5] To describe these systems it is possible to use semi-analytical modeling. Lyman-α systems has been used to constrain different cosmological scenario, see Ref. (McDonald et al. 2004), and references therein. Lyman-α data, which are very sensitive to the matter power spectrum around $k \simeq 10^{-1} - 10^2$ Mpc^{-1}, wavenumbers that are affected by the primordial magnetic field (Shaw & Lewis 2010). As we will see below these systems can be used to place stringent constraints on magnetic field properties.

We do not go through the detailed modeling of Lyman-α systems, leaving this for more precise computations, but we use the direct comparison of the reconstructed matter power spectrum and the theoretical matter power spectra affected by the primordial magnetic field.

For this study we use Lyman-α data obtained by the Keck telescope (Croft 2002). To get a conversion of data points (accounting that we use the wavevector k units h/Mpc, we multiply data by the conversion factor

$$\frac{100\,\sqrt{\Omega_m\,(1+z)^3+\Omega_\Lambda}}{1+z}$$

given in Ref. (Kim et al. 1996). As the data is given at redshift 2.72, we translate the data to redshift zero by multiplying it by the square of the ratio of the growth factor at redshift zero to that at redshift 2.72. We compute the growth factors using the ICOSMOS calculator.[6] Thus, we multiply the data by 8.145 to estimate the Lyman- data at redshift z = 0. The comparison of the theoretical predicted matter power spectrum and Lyman- data is given in Fig. (5).

We use χ^2 statistics to compare the predicted model with Lyman-α data. We assume no correlation between the uncertainties in the $P(\mathbf{k})$ measurements for different $\mathbf{k}$ values and find no evidence for primordial magnetic fields.

The 95% and 68% confidence level limits are given in

[5] These objects have a high column density of neutral hydrogen ($N_{HI} > 10^{20}$cm^{-2}) and are detected by means of absorption lines in quasar spectra (Wolfe 1993). Observations at high redshift have lead to estimates of the abundance of neutral hydrogen in damped Lyman-α systems (Lanzetta et al. 1995). The standard view is that damped Lyman-α systems are a population of protogalactic disks (Wolfe 1993), with a minimum mass of $M = 10^{10}h^{-1}M_{Sun}$ (Haehnelt 1995).

[6] ICOSMOS Calculator is available at http://www.icosmos.co.uk/index.html.

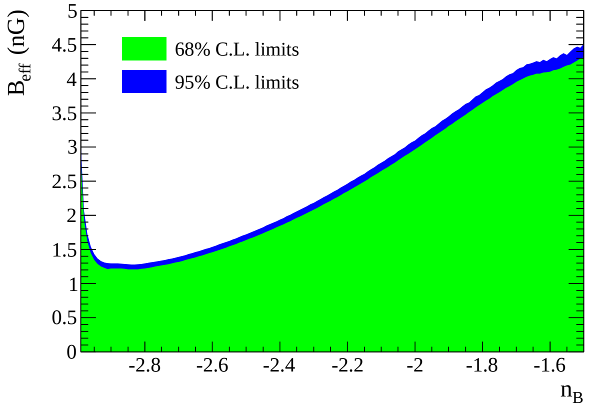

FIG. 6.— The effective magnetic field limits from the lyaman-α data for different values of n_B

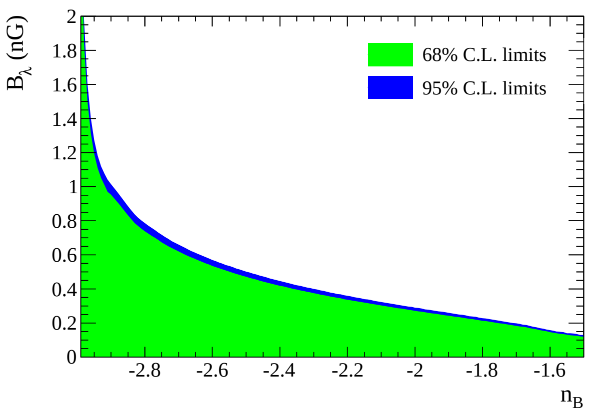

FIG. 7.— The smoothed magnetic field limits from the Lyman-α for different values of n_B

Fig. 6. The limits on B_λ are given Fig. 7. We explicitly present the limits for $B_{\rm eff}$ and B_λ just to show that they have different behaviors when the spectral index is increasing. In terms of the total energy density of the magnetic field the limits are weaker if we are considering the redder spectra. At this point the total energy density of the phase transition generated magnetic field is almost unconstrained.

3.4. *The CMB Faraday Rotation effect*

As we already noted above the primordial magnetic field induces the CMB polarization Faraday rotation, and for an homogeneous magnetic field the rotation angle is given through, (Kosowsky & Loeb 1996)

$$\alpha \simeq 1.6^\circ \left(\frac{B_0}{1\,\mathrm{nG}}\right)\left(\frac{30\,\mathrm{GHz}}{\nu_0}\right)^2, \qquad (8)$$

where B_0 is the amplitude of the magnetic field, and $\nu - 0$ is the frequency of the CMB photons. In the case of the stochastic magnetic field we have to determine the r.m.s. value of the rotation angle, $\alpha_{\rm rms}$, and corresponding expression in terms of the effective magnetic field is given

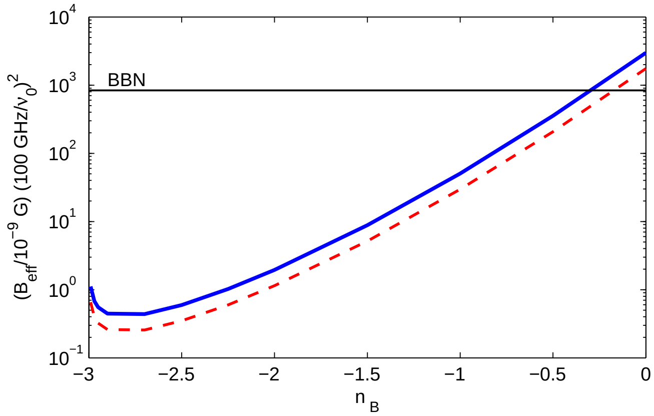

FIG. 8.— The effective magnetic field values for different spectral index $n_{\rm B}$. Solid and dashed lines correspond to the 95% and 68% confidence levels, respectively. Upper limit set by the Big Bang nucleosynthesis $B_{\rm eff} = 840$ nG is shown by horizontal black line (BBN).

in (Kahniashvili et al. 2010), being

$$\alpha_{\rm rms} \simeq 0.14^\circ \left(\frac{B_{\rm eff}}{1\,\mathrm{nG}}\right)\left(\frac{100\,\mathrm{GHz}}{\nu_0}\right)^2 \frac{\sqrt{n_B+3}}{(k_D\eta_0)^{(n_B+3)/2}} \times \left[\sum_{l=0}^{\infty}(2l+1)l(l+1)\int_0^{x_S} dx\, x^{n_B} j_l^2(x)\right]^{1/2}. \qquad (9)$$

Here, η_0 is today value of conformal time, $j_l(x)$ is a Bessel function with argument $x = k\eta_0$, and $x_S = k_S\eta_0$ where $k_S = 2$ Mpc^{-1} is the Silk damping scale. In the case of an extreme magnetic field which just satisfies the BBN bound, k_D might become less than the Silk damping scale. In this case the upper limit in the integral above must be replaced by $x_D = k_D\eta_0$. Note, that for $n_B \to -3$ Eq. (9) is reduced to Eq. (8) (see for details Ref. (Kahniashvili et al. 2010).

Here, we quote Ref. (Komatsu et al. 2010) in order to determine the upper limits for the r.m.s. rotation angle. Adding the statistical and systematic errors in quadrature and averaging over WMAP, QUaD and BICEP (see for details Ref. (Komatsu et al. 2010)) with the inverse variance weighting, it was obtained $\alpha = -0.25^0 \pm 0.58^0$ at (68% CL), or $-1.41^0 < \alpha < 0.91^0$ (95% CL). We obtain for the r.m.s. value (absolute) of the rotation angle $|\alpha_{\rm rms.}| < 0.477^0$ and $|\alpha_{\rm rms}| < 0.997^0$ (68% C.L. and 95% C.L., respectively) assuming gaussian statistics. In Fig. (8) we display the upper limits of the effective magnetic fields using the rotation angle constraints quoted above. Note that these limits order of magnitude better than obtained previously in Ref. (Kahniashvili et al. 2010) where we used the WMAP 7 years data alone. For almost scale-invariant magnetic field the limits are around 0.5 nG. As we can see for $n_B > -0.5$ the BBN limits on the effective magnetic field strength are stronger than those coming from the CMB faraday rotation effect. The situation is completely different when determining the limits for the smoothed magnetic field $B_{\lambda=1\rm Mpc}$ with $n_B > -2$, which are extremely strong from BBN (Caprini & Durrer 2001; Kahniashvili et al. 2011), and moderate in the case of the large scale structures or the CMB birefrigence, see above.

4. CONCLUSION

In this paper we study the large-scale signatures of cosmological magnetic fields, such as the thermal Sunyaev-Zel'dovich effect, halo number density, and Lyman-α data. Due to several uncertainties present in tSZ and halos abundance tests we find that Lyman-α measurements provide the tightest constraints on the primordial magnetic field energy density. We express these limits in terms of the effective value of the magnetic field, $B_{\rm eff}$. In the case of the scale invariant spectrum $n_B = -3$ these limits are identical to limits on the smoothed magnetic field B_λ, (smoothed over a length scale λ that is conventionally taken to be 1 Mpc). For a steep magnetic field with spectral index $n_B = 2$ the difference between the limits derived in terms of the effective and smoothed field is several orders of magnitude. Also limits have different behavior with increasing of n_B. At this point, as we underlined previously (Kahniashvili et al. 2010) using the smoothed magnetic field can result in some confusion: the smoothed magnetic field at 1 Mpc scales is extremely small, while the total energy density of the magnetic field is maximal allowed by BBN bounds. The small values of the magnetic fields for $n_B = 2$ (that corresponds to the phase transition generated magnetic fields) might be treated as non-relevance on these fields. For example, in Ref. (Shaw & Lewis 2010) it is claimed that the magnetic field with the spectral index greater than -2.5 is excluded (Shaw & Lewis 2010), while as it is shown in Ref. (Kahniashvili et al. 2011) the magnetic field with extremely small smoothed field value B_λ at $\lambda = 1$ Mpc order of 10^{-29} Gauss with the spectral index $n_B = 2$ can leave observable traces on the CMB and large scale structure formation. The limits are ranging between 1.5 nG and 4.5 nG for $n_B \in (-3; -1.5)$. These limits are comparable for those from the CMB polarization plane rotation.

Note when this paper was in final stage of preparation Ref. (Pandey & Sethi 2012) appeared showing that at the magnetic field can be strongly constrained by the first object formation, in particular through the Lyman-α data.

We are greatly thankful to R. Shaw for useful comments and discussion. The computation of the magnetic field power spectrum has been performed using the modified version of CAMB, for details see (Shaw & Lewis 2010). We appreciate useful discussions with A. Brandenburg, L. Campanelli, R. Croft, R. Durrer, A. Kosowsky, A. Kravtsov, F. Miniati, B. Ratra, U. Seljak, S. Sethi, and R. Sheth. We acknowledge partial support from Swiss National Science Foundation SCOPES grant 128040, NSF grants AST-1109180, NASA Astrophysics Theory Program grant NNXlOAC85G. T.K. acknowledges the ICTP associate membership program. A.N and N.B. are supported by a McWilliams Center for Cosmology Postdoctoral Fellowship made possible by Bruce and Astrid McWilliams Center for Cosmology. A.T. acknowledges the hospitality of the McWilliams Center for Cosmology.

REFERENCES

Arlen, T. C., Vassiliev, V. V., Weisgarber, T., Wakely, S. P., and Shafi, S. V., arXiv:1210.2802 [astro-ph.HE].

Arnaud, M, Pratt, G. W., Piffaretti, R., Boehringer, H., J. H. Croston, J. H., and Pointecouteau, E., 2010, Astron. and Astrophys., **517**, A92.

Banerjee, R., and Jedamzik, K. 2004, Phys. Rev. D, 70, 123003.

Banerjee, R., and Jedamzik, K. 2003, Phys. Rev. Lett., 91, 251301.

Battaglia, N., Bond, J. R., Pfrommer, C., Sievers, J. L., and Sijacki, D., 2010, Astrophys. J. **725**, 91.

Battaglia, N., Bond, J. R., Pfrommer, C., and Sievers, J. L., 2012, Astrophys. J. **758**, 75.

Beck, R., Brandenburg, A., Moss, D., Shukurov, A., & Sokoloff, D. 1996, ARA&A, 34, 155

Bernet, M. L., Miniati, F., Lilly, S. J., Kronberg, P. P., and Dessauges-Zavadsky, M., 2008, Nature **454**, 302.

Biskamp, D. 2003, *Magnetohydrodynamic Turbulence* (Cambridge University, Cambridge);

Blasi, P., S. Burles, S., Olinto, A. V., 1999, Astrophys. J. **514**, L79.

Brandenburg, A., Enqvist, K., and Olesen, P. 1996, Phys. Rev. D, 54, 1291.

Broderick, A. E., Chang, P., and Pfrommer, C., 2012, Astrophys. J. **752**, 22.

Burenin, R. A. and Vikhlinin, A. A., 2012, Astron. Lett. **38**, 347.

Caprini, C., and Durrer, R., 2001, Phys. Rev. D. **65** 023517.

Croft, R. A. C., *et al.*, (2002) Astron. Astrophys. **581**, 20.

Dermer, C. D., Cavaldini, M., Razzaque, S., Finke, J.D., Chiang, J., Lott, B., 2011 ApJ733, L21.

Dolag, K., Bartelmann, M., and Lesch, H. 2002, A&A, 387, 383

Dolag, K., Kachelriess, M., Ostapchenko, S. and Tomas, R., 2011, ApJ727, L4.

Dunkley, J., Hlozek, R., Sievers, J., Acquaviva, V., Ade, P. A. R. Aguirre, P., Amiri, M., and Appel, J. W., *et al.*, 2011, Astrophys. J. **739**, 52.

Durrer, R. and Caprini, C. 2003, J. Cosmology Astropart. Phys., 0311, 010.

Fang, T., Humphrey, P. J., and Buote, D. A., 2009, Astrophys. J. **691**, 1648.

Gopal, R. and Sethi, S. K., 2005 Phys. Rev. D **72**, 103003.

Grasso D. and H.R. Rubinstein, H. R., 2001, Phys. Rev. D348, 163.

Haehnelt, M.G., 1995, Mon. Not. Roy. Astron. Soc. **273** , 249.

Hogan, C. J. 1983, Phys. Rev. Lett., 51, 1488.

Hu, W. and Kravtsov, A., 2003, Astrophys. J. 584, 702.

Jedamzik, K., Katalinic, V., and Olinto, A. V, 1998 Phys. Rev. D **57**, 3264.

Jenkins, A. and Frenk, C. S. and White, S. D. M. and Colberg, J. M. and Cole, S. and Evrard, A. E. and Couchman, H. M. P. and Yoshida, N., 2001, Mon. Not. Roy. Astron. Soc.]bf 321 372.

Kahniashvili, T., Tevzadze, A. G., Sethi, S., Pandey, K., and Ratra, B., 2010, Phys. Rev. D **82**, 083005.

Kahniashvili, T., Tevzadze, A. G., and Ratra, B., 2011, ApJ, 726, 78.

Kandus, A., Kunze, K. E., and Tsagas, C. G., 2011, Phys. Rept. **505**, 1.

Kim, E., Olinto, A. V., and Rosner, R., 1996, Astrophys. J. **468**, 28.

Kim, T. S., *et al.*, 2004, Mon. Not. Roy. Astron. Soc. **347**, 355.

Komatsu, E. and Seljak, U., 2002, cosmological parameters," Mon. Not. Roy. Astron. Soc. **336**, 1256.

Komatsu, E., et al. [WMAP Collaboration] 2011, Astrophys. J. Suppl. **192**, 18.

Kosowsky, A. and Loeb, A., 1996, Astrophys. J. **469**, 1.

Kravtsov, A. and Borgani, S. 2012, Annual Rev. of Astron. and Astrophys., **50**, 353.

Kronberg, P. P., M. L. Bernet, M. L., Miniati, F., Lilly, S. J., Short, M. B., and Higdon, D. N., 2008, Astrophys. J, **676**, 70.

Kulsrud, R. M. and Zweibel, E. G., 2008, Rept. Prog. Phys. **71**, 0046091.

Lanzetta, K.M., Wolfe, A.M. and Turnshek, D.A. 1995, Astrophys. J **440**, 435.

Lueker, M., Reichardt, C. L., Schaffer, K. K., Zahn, O., Ade, P. A. R., Aird, K.A., Benson, B. A., and Bleem L. E., *et al.*, 2010, Anisotropies with the South Pole Telescope," Astrophys. J. **719**, 1045.

Mack, A., Kahniashvili, T., and Kosowsky, A., 2002, Phys. Rev. D **65**, 123004.

McDonald, P, Seljak, U., Cen, R., Shih, D., Weinberg, D. H., Burles, S., Schneider, D. P., Schlegel, D. J., Bahcall, N. A., Briggs, S. W. et al., 2005, Astrophys. J. **635**, 761,

Neronov, A., and Vovk, I., 2010, Science **328**, 73.

Pandey K. L. and Sethi, S. K., 2012 arXiv:1210.3298 [astro-ph.CO].

Press, W. H., and Schechter, P., 1974, Astrophys. J. **187**, 425.

Reichardt, C. L., Shaw, L., Zahn, O., , Aird, K. A., Benson, S. A., Bleem, L. E., J. E. Carlstrom, J. E., and C. L. Chang C. L., *et al.*, 2012, anisotropies with two years of South Pole Telescope observations," Astrophys. J. **755**, 70.

D. R. G. Schleicher and F. Miniati, 2011, Mon. Roy. Not Ast. Soc. **418** L143.

Shaw, L. D. Nagai, D., Bhattacharya, S., and Lau, E. T., 2010, Astrophys. J. **725**, 1452.

Shaw, J. R. and A. Lewis, A., 2012, Phys. Rev. D **86**, 043510.

Sheth, R. K. and Tormen, G., 1999, Mon. Not. Roy. Astron. Soc. **308**, 119.

Springel, V., 2010, Ann. Rev. Astron. Astrophys. **48**, 391.

Subramanian, K. and Barrow, J. D., 1998, Phys. Rev. D **58**, 083502.

Subramanian, K., Shukurov, A., and Haugen, N. E. L. 2006, Mon. Not. Roy. Astron. Soc. **366**, 1437.

Tavecchio, F., Ghisellini, G., Foschini, L., Bonnoli, G., Ghirlanda, G., and Coppi,P., 2010, Mon. Not. Roy. Astron. Soc. **406**, L70.

Trac, H., Bode, P., and Ostriker, J. P., 2011, Astrophys. J. **727**, 94.

Vallée, J. P. 2004, New Astron. Rev., 48, 763.

Vazza, F., Tormen, G., Cassano, F., Brunetti, G., and Dolag, K., 2006, Mon. Not. Roy. Astron. Soc. Lett. **369**, L14.

Yamazaki, D. G., Ichiki, K,, Kajino, T., and Mathews, G. J., 2012, Adv. Astron. **2010**, 586590.

White, M., 2001, Astron. Astrophys. **367**, 27.

White, M. 2002, Astrophys. J. Supl. **143**, 241.

Widrow, L. M. 2002, Rev. Mod. Phys., 74, 775.

Wolfe, A., 1993, in *Relativistic Astrophysics and Particle Cosmology* , eds. C.W., Ackerlof, M.A., Srednicki (New York: New York Academy of Science) , p.281